Lecture Notes in Mechanical Engineering

Muhammad Yusri Ismail
Mohd Shahrir Mohd Sani
Sudhakar Kumarasamy
Mohd Adnin Hamidi
Mohd Shamil Shaari *Editors*

Technological Advancement in Mechanical and Automotive Engineering

Proceeding of International Conference in Mechanical Engineering Research 2021

Springer

Lecture Notes in Mechanical Engineering

Lecture Notes in Mechanical Engineering (LNME) publishes the latest developments in Mechanical Engineering—quickly, informally and with high quality. Original research reported in proceedings and post-proceedings represents the core of LNME. Volumes published in LNME embrace all aspects, subfields and new challenges of mechanical engineering. Topics in the series include:

- Engineering Design
- Machinery and Machine Elements
- Mechanical Structures and Stress Analysis
- Automotive Engineering
- Engine Technology
- Aerospace Technology and Astronautics
- Nanotechnology and Microengineering
- Control, Robotics, Mechatronics
- MEMS
- Theoretical and Applied Mechanics
- Dynamical Systems, Control
- Fluid Mechanics
- Engineering Thermodynamics, Heat and Mass Transfer
- Manufacturing
- Precision Engineering, Instrumentation, Measurement
- Materials Engineering
- Tribology and Surface Technology

To submit a proposal or request further information, please contact the Springer Editor of your location:

China: Ms. Ella Zhang at ella.zhang@springer.com
India: Priya Vyas at priya.vyas@springer.com
Rest of Asia, Australia, New Zealand: Swati Meherishi at swati.meherishi@springer.com
All other countries: Dr. Leontina Di Cecco at Leontina.dicecco@springer.com

To submit a proposal for a monograph, please check our Springer Tracts in Mechanical Engineering at https://link.springer.com/bookseries/11693 or contact Leontina.dicecco@springer.com

Indexed by SCOPUS. All books published in the series are submitted for consideration in Web of Science.

More information about this series at https://link.springer.com/bookseries/11236

Muhammad Yusri Ismail ·
Mohd Shahrir Mohd Sani · Sudhakar Kumarasamy ·
Mohd Adnin Hamidi · Mohd Shamil Shaari
Editors

Technological Advancement in Mechanical and Automotive Engineering

Proceeding of International Conference in Mechanical Engineering Research 2021

Springer

Editors
Muhammad Yusri Ismail
Faculty of Mechanical and Automotive Engineering Technology (FTKMA)
Universiti Malaysia Pahang
Pekan, Malaysia

Sudhakar Kumarasamy
Faculty of Mechanical and Automotive Engineering Technology (FTKMA)
Universiti Malaysia Pahang
Pekan, Malaysia

Mohd Shamil Shaari
Faculty of Mechanical and Automotive Engineering Technology (FTKMA)
Universiti Malaysia Pahang
Pekan, Malaysia

Mohd Shahrir Mohd Sani
Faculty of Mechanical and Automotive Engineering Technology (FTKMA)
Universiti Malaysia Pahang
Pekan, Malaysia

Mohd Adnin Hamidi
Faculty of Mechanical and Automotive Engineering Technology (FTKMA)
Universiti Malaysia Pahang
Pekan, Malaysia

ISSN 2195-4356 ISSN 2195-4364 (electronic)
Lecture Notes in Mechanical Engineering
ISBN 978-981-19-1456-0 ISBN 978-981-19-1457-7 (eBook)
https://doi.org/10.1007/978-981-19-1457-7

This Springer imprint is published by the registered company Springer Nature Singapore Pte Ltd.
The registered company address is: 152 Beach Road, #21-01/04 Gateway East, Singapore 189721, Singapore

Preface

It is our great pleasure to present the compilation of Proceedings of International Conference in Mechanical Engineering Research (ICMER 2021). The 6th conference in mechanical engineering research is hosted by Faculty of Mechanical and Automotive Engineering Technology (FTKMA) in collaboration with Ningxia University of China, Universiti Teknologi Malaysia (UTM), UCSI University and the University of Mindanao.

ICMER 2021 is a scientific forum of discussion for scientists, researchers and engineers from all over the world to exchange ideas and the research results in the field of automotive technology, advanced fluid, advanced material, energy management and advanced manufacturing.

This conference is the first conference in the history of international conference in mechanical engineering research conducted in virtual through online platform due to the COVID-19 pandemic that hits across the globe. Therefore, we would like to express our sincere appreciation and gratitude to the committee members, co-organizer and reviewers to make this conference successful.

Last but not least, we would like to thank the keynote speakers and participants who contributed their knowledge to this prestigious conference.

Pekan, Malaysia

Muhammad Yusri Ismail
Corresponding Editor

Contents

Automotive Technology

Finite Element Analysis of Automotive Door Hinge 3
M. I. Hadi, M. R. M. Akramin, and M. S. Shaari

Graphene as an Alternative Additive in Automotive Cooling System 13
Ganesaan Kadirgama, Muhammad Izdihar Bin Razman, Devarajan Ramasamy, Kumaran Kadirgama, and Kaniz Farhana

A Review on Torque Performance for Different Type of Carrier Fluid in Magnetorheological Brake 37
Khairul Anwar Abdul Kadir, Nurhazimah Nazmi, Shinichirou Yamamoto, Saiful Amri Mazlan, Nur Azmah Nordin, and Shahir Mohd Yusuf

Study of Engine Performance, Emission and Combustion of Reactivity Controlled Compression Ignition (RCCI) Mode Engine 51
M. Jamil, M. A. Hamidi, A. F. Yusop, M. F. Zakiyuddin, and M. N. Omar

Effect of Primary Reference Fuel on Reactivity-Controlled Compression Ignition Engine Emission Produce 65
M. F. Zakiyuddin, Muthanna Jamil, M. A. Hamidi, and A. F. Yusop

Emission Characteristics Effect on Rice Bran Oil Enriched with Diesel Fuel on Compression Ignition Engine 75
M. Norhafana, C. K. Ihsan, M. M. Noor, A. A. Hairuddin, K. Kadirgama, and D. Ramasamy

The Performance of Beta Type Stirling Engine Using Different Fuel 89
X. H. Ng, R. A. Bakar, K. Kadirgama, Sivaraos, D. Ramasamy, and M. Samykano

Dual Fuel Soy Biodiesel and Natural Gas Swirl Combustion for Toxic Emissions Reduction 111
Meng-Choung Chiong, Guo Ren Mong, Keng Yinn Wong, Hui Yi Tan, and Nor Afzanizam Samiran

Design and Analysis of Composite Materials for Vehicle Engine Mount 121
A. R. Abd Hamid and T. M. Chin

Experimental Investigation of a Diesel Engine Using Waste Plastic Oil Blends 133
A. M. Norkhizan, A. F. Yusop, and M. A. Hamidi

Biocrude Potential Assessment of Macroalgae for Sustainable Biofuel Production 145
Nida Khan, K. Sudhakar, and R. Mamat

Advanced Fluid

Thermal–Hydraulic Performance of Water: Ethylene Glycol Mixture Through Guide-Vane Swirl Generator: A Numerical Simulation 159
M. A. At-Tasneem, W. H. Azmi, and M. A. Ismail

Photodegradation of Biobased Oils Polymer Blended with High Density Polyethylene upon Ultraviolet Irradiation Exposure 171
Nurulsaidatulsyida Sulong, Anika Zafiah Mohd Rus, Nurul Syamimi Mohd Salim, Nik Normunira Mat Hassan, and Noraini Marsi

Effects of Solvents on ZnO Nanoparticles Synthesis via Sol–gel Method 181
Suraya Sulaiman, Nur Syazwa Zamri, Radhiyah Abd Aziz, Mohamad Farid Mohamad Sharif, Natasha Ahmad Nawawi, and Nur Ayuni Jamal

A Comparative Study and ANSYS Simulation on Thermal Performance of Shell and Tube Heat Exchanger Operated with Al_2O_3-Water and TiO_2-Water Nanofluids 191
U. Z. A. Rahman, A. S. A. Abdelhamid, and Mohammed W. Muhieldeen

Classification of Lubricants Base Oils for Nanolubricants Applications—A Review 205
G. Kadirgama, Mohd Kamal Kamarulzaman, D. Ramasamy, K. Kadirgama, and Sakinah Hisham

An Experimental Evaluation of Specific Heat of Mono and Hybrid Nanofluids 215
Kaniz Farhana, Kumaran Kadirgama, Danial Mohamed, Abu Shadate Faisal Mahamude, Sivarao Subramonian, Devarajan Ramasamy, and Mahendran Samykano

Preparation and Characterization of Cross-Linked Chitosan/Cellulose Bionanohybrids 225
Mostafa Yusefi, Kamyar Shameli, Justin Chan Zhe, and Nor Azwadi Bin Che Sidik

Effect of Catalyst in the Pyrolysis of Waste Polyethylene Terephthalate (PET) Plastics 237
Emil Jean D. Loreniana, Justin Dhavee D. Sorongon, and Cresencio P. Genobiagon Jr.

Advanced Material

Optimization of WC-Tac-Co for Green Porosity via Metal Injection Moulding 251
Siti Nur Fatimah Khairudin, Hazriel Faizal Pahroraji, Siti Khadijah Alias, and Mohd Halim Irwan Ibrahim

The Change of Solidification Parameters on Hypoeutectic Aluminum–Silicon Alloy Under Different Cooling Rates 263
X. H. Ma and N. A. Abd Razak

A Brief Overview on the Utilization of High Strength Steel (HSS) for Automotive Structural Welding Applications 279
M. N. M. Salleh, M. Ishak, and M. M. Quazi

Evaluation of Tin Slag Polymer Concrete Column Compressive Behavior Using Finite Element Analysis 289
M. S. Manda, M. R. M. Rejab, and Shukur Abu Hassan

Creep Life Prediction of P91 Steel Using Omega Method 303
S. N. A. Rosli, N. Ab Razak, M. R. Mahazar, and N. A. Alang

Effect of Cavity Thickness on Copper Alloy Corrosion Resistance 315
M. Nasuha, M. M. Rashidi, A. Hadi, Z. Shayfull, and T. M. Sheng

pH-Responsive Nanocapsules as Smart Coating for Corrosion Protection: A Review 329
N. S. Mohamed, J. Alias, N. A. Johari, and A. Zanurin

Effect of Artificial Aging on the Microstructure and Mechanical Properties of AJ62 Magnesium Alloys 339
M. I. M. Ramli, M. A. F. Romzi, J. Alias, and N. A. Abd Razak

Microstructural and Mechanical Characterization of AlSi10Mg Additively Manufactured Material Using Direct Metal Laser Sintering Technique 349
S. P. Tan, M. A. Ramlan, M. S. Shaari, Akiyuki Takahashi, and M. R. M. Akramin

Quenching Heat Transfer Characteristics of Copper Rod in Saturated and Various Subcooled Condition 361
H. Zeol, M. Z. Sulaiman, H. Z. Hui, H. Ismail, and T. Okawa

The Effect of Trawl Activities to Subsea Pipelines of East Coast Peninsular Malaysia: A Risk Analysis 379
Ahmad Faizal Ahmad Fuad, Mohd Hafizi Said, Khalid Samo, Mohd Hairil Mohd, Fatin Alias, and Mohd Asamudin A. Rahman

Effect of Pullulan Amount on ZnO NPs Via Sol–Gel Technique 391
Eleen Dayana Mohamed Isa, Kamyar Shameli, Nurfatehah Wahyuny Che Jusoh, Roshasnorlyza Hazan, and Nor Azwadi Che Sidik

Effect of Porosity and Permeability Characteristics on the Silver Catalyst of the Hydrogen Peroxide Monopropellant Thruster Performances 399
Muhammad Shahrul Nizam Shahrin, Norazila Othman, Nik Ahmad Ridhwan Nik Mohd, and Mastura A. B. Wahid

Numerical Simulation of the Effect of Surface Roughness on the Throttling Characteristics for Multi-stage Pressure Reducing Valves 417
Guan Wang, Jianfei Deng, Linyuan Kou, and Xuejun Zhu

Influence of Temperature and pH Value in 3.5% NaCl Solution on Electrochemical Performance of 316L Stainless Steel 429
G. Wang, Z. K. Zou, P. Zhang, Y. Wu, L. Y. Kou, and Y. Q. Xu

The Influence of Coal Water Slurry Particle Size on the Erosion of Reducing Pipe 441
G. Wang, Q. F. Gao, J. F. Deng, W. H. Wang, Y. X. Zhang, X. J. Zhu, and Y. Q. Xu

Study on Nozzle Baffle in Shield Machine Remote Pressure Maintaining System 457
G. Wang, Y. X. Zhang, Z. C. Wu, L. Y. Kou, X. Shang, Q. F. Gao, W. H. Wang, and Y. Q. Xu

Geometry and Kinematics Analysis of Seven-Bar Three-Axis Fixed Compound Mechanism 471
Xing Zhenwei and Wang Yutan

Energy Management

Economic Analysis Comparison Between Payback Period and Net Present Value for Office Building Energy Consumption 487
Z. Noranai, N. M. Sobri, and M. Z. M. Bosro

A Kinetic Mechanism Based on Lens Law Concept of Hybrid Generator 497
Saiful Bahari Shaari, Zulkifli Mohamed, and Hanif Ramli

Performance Testing of Pico Hydropower Turbine Prototype 507
Hema Vharman Ganasan, Mohd Zarhamdy Md Zain, Mastura Ab Wahid, Mohamed Hussein, and Azman Jamaludin

Unsteady Free Convection with Volumetric-Radiation Using LBM 519
Raoudha Chaabane, Abdelmajid Jemni, Nor Azwadi Che Sidik, and Hong Wei Xian

Numerical Study of Magneto-hydrodynamic Free Convection Heat Transfer and Fluid Flow 547
Raoudha Chaabane, Abdelmajid Jemni, Nor Azwadi Che Sidik, and Hong Wei Xian

Microwave Hybrid Heating as an Alternative Method for Soldering—A Brief Review 565
N. M. Maliessa and S. R. A. Idris

Effect of Opening Ratios with and Without Louvers in Cross Ventilation Using CFD 579
Lip Kean Moey, Saleh Mohammed Saleh Alyazidi, Vin Cent Tai, Joseph Wu Kai-Seun, Prasath Reuben Mathew, and Ahmed Nurye Oumer

Applications of Graphene Nanomaterials in Energy Storage—A State-of-Art Short Review 595
Kaniz Farhana, Kumaran Kadirgama, Sivarao Subramonian, Devarajan Ramasamy, Mahendran Samykano, and Abu Shadate Faisal Mahamude

Enhanced Smoke Wire Technique with Control Dripping Valve in a Small Scaled Quasi-atmospheric Boundary Layer Wind Tunnel 611
Nurizzatul Atikha Rahmat, Mohammad Rozaki Ramli, Mujahid Husaimi Che Hassan, Kamil Khalili Haji Abdullah, and Khairun Adhani Khairunizam

A Numerical Simulation of Heat Transfer Characteristic of Twisted Tube in an Annular Heat Exchanger 629
Abdallah Talal Banat, Teng Kah Hou, Tey Wah Yen, I. A. Idowu, and Mohammed W. Muhieldeen

Study on the Effects of Tube Arrangements to the Heat Transfer Performance of Evaporator Chiller System Based on Industrial Standards 641
Hamad Ali Hamad Bin Hatrash, Ir. Noor Idayu Binti Mohd Tahir, and Mohammed W. Muhieldeen

Effect of Air Filter Pressure on Fuel Consumption and Cost of Gas Turbine in Southern Power Generation, Malaysia 655
A. H. Fauzi and M. Z. Sulaiman

Simulated Performance of an Improved District Cooling System (DCS) in Tronoh, Perak, Malaysia 669
Jue Hao Teo, J. C. E. Yong, Mohammed W. Muhieldeen, J. Y. Chan, A. G. Olasunkanmi, and C. L. Siow

Polyethylene Bubble Aluminium SB250-FR+ for Reduced Energy Consumption Building: An Experimental Study 685
Mateus De Sousa, Mohammed W. Muhieldeen, Jayden Lau, Wah Yen Tey, Teng Kah Hou, and U. Z. A. Rahman

Improvements of the Cyclone Separator Performance for Wood Waste Combustion by an Aggregation Chamber 695
Charlito L. Cañesares

Soil Characteristic Study to Improve Heat Conductivity Capability in Ground Heat Exchanger 707
A. M. Aizzuddin, A. A. Asrudin, T. M. Yusof, and W. H. Azmi

Boiler Efficiency Analysis Using Direct and Indirect Method 721
Wan Mohd Fakhri Wan Zainus and Natrah Kamaruzaman

A Review of Active Day Lighting System in Commercial Buildings with the Application of Optical Fiber 731
Lokesh Udhwani and Archana Soni

Numerical Simulation and Flow Characteristic Analysis of Labyrinth Control Valve 753
G. Wang, W. H. Wang, J. F. Deng, Q. F. Gao, Y. X. Zhang, S. Y. Bao, X. J. Zhu, and N. N. Gou

Advanced Manufacturing

A Scrum-Based New Product Introduction (NPI) in Contract Manufacturing 767
Ang Chee Yiang, Chin Jeng Feng, and Nur Amalina binti Muhammad

End-Mill Carbide Tool Wear in Machining Metallic Biomaterial 783
Azli Ihsan Yahaya, Saiful Anwar Che Ghani, Daing Mohamad Nafiz Daing Idris, and Mohd Azwan Aziz

Defect Identification During Pulse Mode Laser Welding Process Through the Pattern Recognition Analysis of the Acquired Sound Frequency Spectrum 793
M. F. M. Yusof, M. Ishak, M. N. Salleh, and M. F. Ghazali

Effect of Laser Micro-drilling Parameters on Hole Geometry and Hole Formation of Thin Sheet SS304 803
M. S. Haneef, G. H. Lau, M. H. Aiman, M. M. Quazi, and M. Ishak

A Simulation Study on Interfacial Reaction Between Sn3Ag0.5Cu and Sn0.7Cu Using Different Substrates After Reflow Soldering 815
M. H. Mohd Zaki and S. R. A. Idris

Investigation of Opening Position on Natural Cross Ventilation for an Isolated Building 825
Lip Kean Moey, Rui Jun Tok, Vin Cent Tai, Prasath Reuben Mathew, Joseph Wu Kai-Seun, and Ahmed Nurye Oumer

Effect of Laser Frequency and Focal Length on Copper Surface Temperature During Laser Heating 839
M. Y. Yus Erny, A. Afiq, M. H. Aiman, M. M. Quazi, and M. Ishak

Surface Roughness Analysis of Five-Axis Flank Milling Strategies for Slanted Thin-Walled Pocketing: Aerospace Part 847
S. A. Sundi, R. Izamshah, M. S. Kasim, I. S. Othman, and M. R. Raffay

Using X-Ray Computed Tomography for Effective Porosity Characterisation in Additively Manufactured Metallic Parts 859
Shahir Mohd Yusuf, Nor Azwadi Che Sidik, and Nong Gao

Effect of Sn-*x*Cu Solder Alloy onto Intermetallic Formation After Laser Soldering 869
M. A. Abdullah and S. R. A. Idris

Effect of Particle Discretisation and Horizon Size on the Displacement and Damage Plot Using Bond-Based Peridynamics 881
H. N. Yakin, N. Nikabdullah, and M. R. M. Rejab

The Effect of Laser Power and Laser Scan Passes on Bending Angle of Stainless Steel AISI 304 Laser Bending 899
N. Affaf, H. S. Wong, M. H. Aiman, M. Ishak, and M. M. Quazi

A Short Review on Grain Refinement Techniques in Semisolid Metal Processing 909
M. A. Shakirin, N. A. Abd Razak, and A. H. Ahmad

Review on Thermodynamic Properties of Plastic by Fused Deposition Modeling 919
Xinglong Shi, Wenjie Ding, Qianjin Wang, Tongman Li, and Nan Zhao

Research on Operation Data Mining of Pulse Dust Collector 935
Qianjin Wang, Wenbo Han, Wenjie Ding, Wenchuan Ding, and Yongzhu Li

A Study on Tooling Design Procedure for Modeling a Vehicle Part and Its Mold Using CAD/CAM System 947
Mohd Azuwan Ramli and Mohd Salman Abu Mansor

Effect of Laser Surface Modification on SS316L Surface Roughness and Laser Heating Temperature 959
A. Q. Zaifuddin, M. D. Afiq, M. H. Aiman, M. M. Quazi, and M. Ishak

Development of Cooling Necklace System Using Vortex Tube 971
Amirul Nawaf Esa, Mohd Hazwan Yusof, Deyerbeen Sipaan Fredoline, and Muhammad Fadhli Suhaimi

Automotive Technology

Finite Element Analysis of Automotive Door Hinge

M. I. Hadi, M. R. M. Akramin, and M. S. Shaari

Abstract Door hinges and latches are door retention mechanism elements that play an important role in automobiles by holding the door open in the event of a side impact or rollover collision. Hinges are a group of components that are attached to the vehicle's door and frame, are related to one another, and can rotate along the same axis. Latches are mechanical devices that are used to position the door in a closed position relative to the vehicle body while allowing for controlled release. The standard specific conditions for side door latches and hinges installed on cars to reduce the risk of passengers being thrown out of the vehicle as a result of any impact. The objective of this paper is to identify the weakest point and to perform a structural analysis of automotive door hinge. Computer Aided Design (CAD) software is used to build a CAD model of the hinge and lock. The models of such components is meshed, and boundary conditions is defined, using the commercial meshing program. ANSYS is used to analyses the structural behaviour. Based on the results, the component will be further optimized for the future work.

Keywords Car door hinge · FEA · FEM

1 Introduction

The door hinges allow the car or the doors of the truck to be opened or closed. That is where the door fits on the frame [1]. Each door has two hinges, a upper hinge and a lower hinge. There is a circular pin inside the hinge which enables the hinge to swing around the pin axis [2]. Car hinges and door locks are elements of door retention [3]. Hinge has the capacity to rotate along the same axis and is an assembly made up of components attached to the vehicle's body and the door [4]. For the car locking, nowadays is equipped with two places latch mechanism. First one is 'fully latched position' and the second is 'latched position' [5].

M. I. Hadi · M. R. M. Akramin (✉) · M. S. Shaari
Faculty of Mechanical & Automotive Engineering Technology (FTKMA), Universiti Malaysia Pahang, 26600 Pekan, Pahang, Malaysia
e-mail: akramin@ump.edu.my

M. Y. Ismail et al. (eds.), *Technological Advancement in Mechanical and Automotive Engineering*, Lecture Notes in Mechanical Engineering,
https://doi.org/10.1007/978-981-19-1457-7_1

Table 1 Total ejections: 1995–2003 NASS and FARS report, on an annual basis

	Total occupants	Unejected	All ejection
All crashes	5,023,879	4,969,797	54,082
Rollover	444,267	410,420	33,847
Non-rollover	4,576,612	4,559,377	20,235

The first challenge is to predict the number of deaths in a single year if all vehicles on the road were constructed using prior technologies. On the basis of the 1995–2003 data from the National Automotive Sampling System (NASS) and the FAA (FARS), 5,023,879 vehicle passengers were involved in car accidents on an annual basis. Vehicle expelled occupants carried 54,082 as shown in Table 1. In ejections where the path of ejection was identified, 59% occurred through side glazing and 26% occurred through openings other than side glazing or doors (i.e., convertible tops, sunroofs, windshields, open truck beds). The others, 15%, took place at the door of a truck. The rate of expulsion by doors depends strongly on the occupant's use of the seatbelt. Unbelted occupants account for 94% of door ejections and if it seems to be a small amount (54,082 people about1.08%), i.e. a small number of people being killed as a result of opening a door due to damage [6], it is also very significant. That life is a valuable commodity. We must save lives in every way possible.

The Federal Motor Vehicle Safety Standard 206 "specify standards for side door locks and side door retaining parts, including latches, hinges, and other supporting means, to reduce the risk of passengers being ejected from the vehicle as a result of impact." Already in the early 1960s, passenger ejection was recognized as the leading cause of death in rollovers and a major problem in other crash modes.

Thus, the objective of this paper is to find stresses and deformation of door hinges under different loading conditions in order to enhance the design. The structural analysis is performed using FEA. FEA is used to simulate the over bending test and identify the weakest point area. Last but not least to recommend appropriate design alternatives for increasing strength and reducing its mass.

2 Finite Element Analysis of Door Hinge

The model of an automotive door hinge was created using the 3D modeling of Computer Aided Design software. It is consisting of three parts which are: a door side bracket, a body side bracket, and a circular pin. Figure 1 shows a model of an automotive door hinge for investigation.

The door hinge is made from a variety of materials, including S.G. iron (ductile iron), aluminum, and mild steel. Mechanical, chemical, and physical properties are three essential parameters for material selection. The aluminum and iron are selected for analysis because of its properties and availability. The physical and mechanical properties of an aluminum and cast-iron door hinge are shown in Table 2.

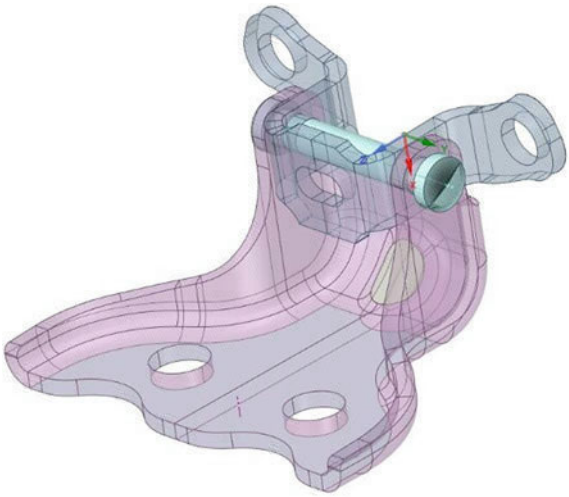

Fig. 1 Modelling of a hinge for an automotive door

The forces are taken from the IS 14225:1995 General specifications for automotive vehicles' locking systems and door retention parts. When a longitudinal load of 11,130 N is added to a door hinge structure, the structure should capable to support the door and undetachable. If the door hinge is subjected to a transverse load of 8930 N, each door hinge mechanism must support the door and undetachable.

The tensile force must be exerted equidistant between the hinge pin's linear core and through the hinge pin's centre line in the longitudinal vehicle direction. According to the original equipment manufacturer, a door hinge assembly must be able to sustain an ultimate normal load of 400 N without breaking. This is based on the door hinge being completely open.

Table 2 Physical and mechanical properties of aluminum door hinge

Properties	Total occupants
Young's Modulus	7.1e + 10 Pa
Density	2770 kg/m^3
Poisson's ratio	0.33
Yield strength	2.8e + 8

Table 3 Physical and mechanical properties of cast iron door hinge

Properties	Total occupants
Young's Modulus	1.1e + 11 Pa
Density	7200 kg/m^3
Poisson's ratio	0.28
Yield strength	8.2e + 8

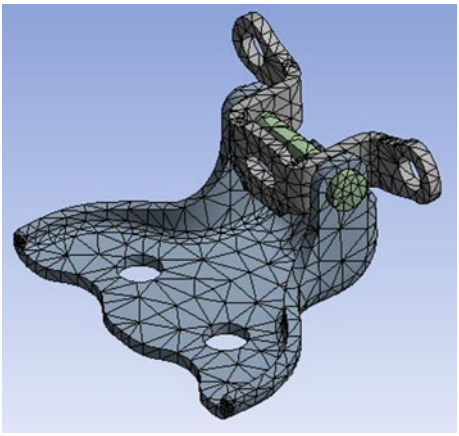

Fig. 2 Mesh of the door hinge

Tables 2 and 3 after the material properties is available, the methodology is shifted to meshing process.

During the meshing process as shown in Fig. 2, the geometry is modelled using .igs file. Later it is imported into FEA software. Once the CAD data for the door hinge structure has been imported, the surfaces of door hinge are developed and meshed. Since all of the dimensions of the door hinge are observable (3D), the part is meshed in a tetra-hedral element.

The forces are taken from the IS 14225:1995 General specifications for automotive vehicles' locking systems and door retention parts. When a longitudinal load of 11,130 N is added to a door hinge structure, the structure should capable to support the door and undetachable. If the door hinge is subjected to a transverse load of 8930 N, each door hinge mechanism must support the door and undetachable.

The tensile force must be exerted equidistant between the hinge pin's linear core and through the hinge pin's centre line in the longitudinal vehicle direction. According to the original equipment manufacturer, a door hinge assembly must be able to sustain an ultimate normal load of 400 N without breaking. This is based on the door hinge being completely open.

3 Results and Discussion

The door hinge is analysed using FEA software. At first, the door hinge is exposed to the maximum normal load on the door panel. The initial design of the door hinge was analysed to determine the maximum stress that would surpass the material's yield strength. Figure 3 shows the total deformation of car door hinge using aluminium. The maximum stress of car door hinge for aluminium is shown in Fig. 4. Figure 5 shows the maximum elastic strain of car door hinge for aluminium. Meanwhile for cast iron, it is shown by Figs. 6, 7 and 8.

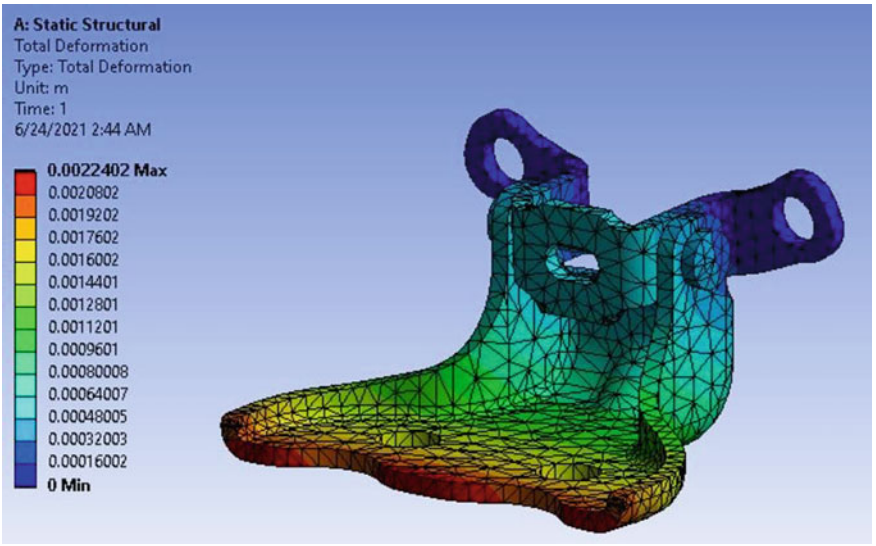

Fig. 3 Total deformation of car door hinge for aluminum

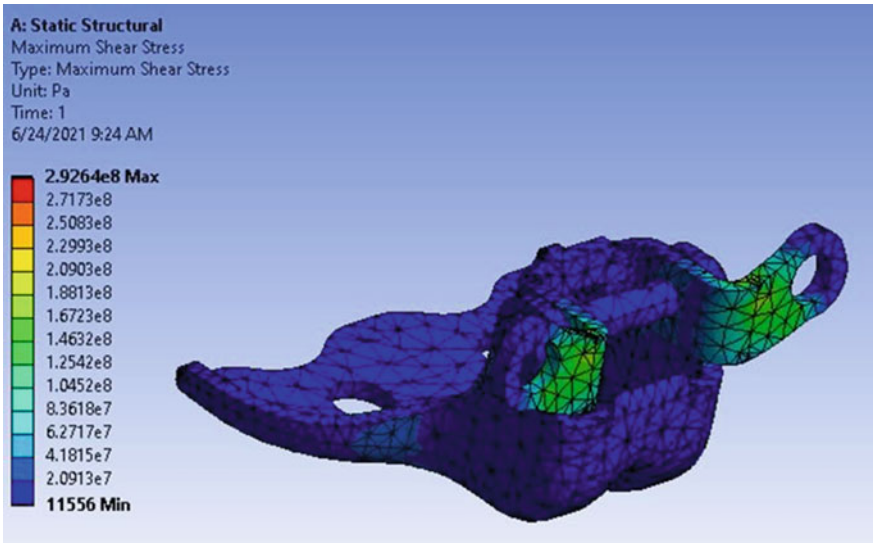

Fig. 4 Maximum stress of car door hinge for aluminum

Maximum deformation of door hinge under extreme condition is 0.22202 mm and maximum stress produced in 2.9264×10^8 Pa for aluminium. For cast iron the maximum deformation of door hinge under extreme condition is 0.14293 mm and maximum stress produced in 3.0105×10^8 Pa.

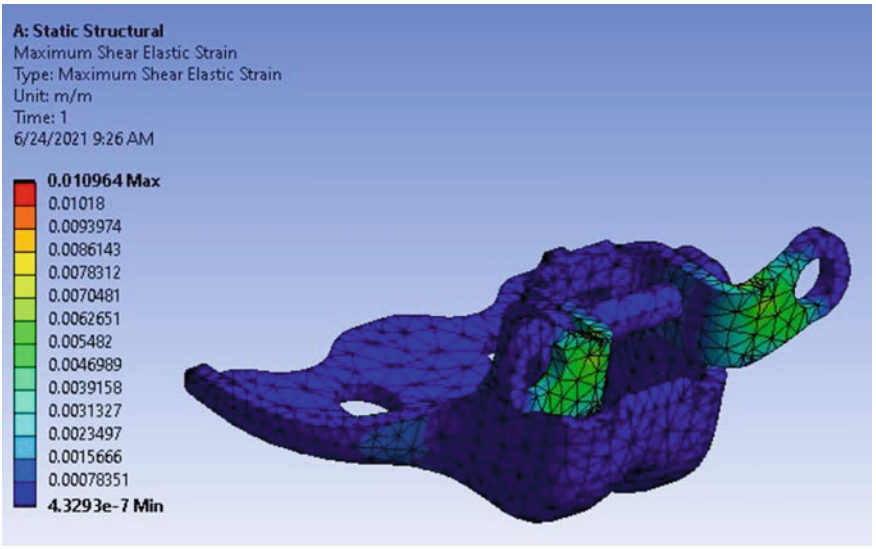

Fig. 5 Maximum elastic strain of car door hinge using aluminum material.

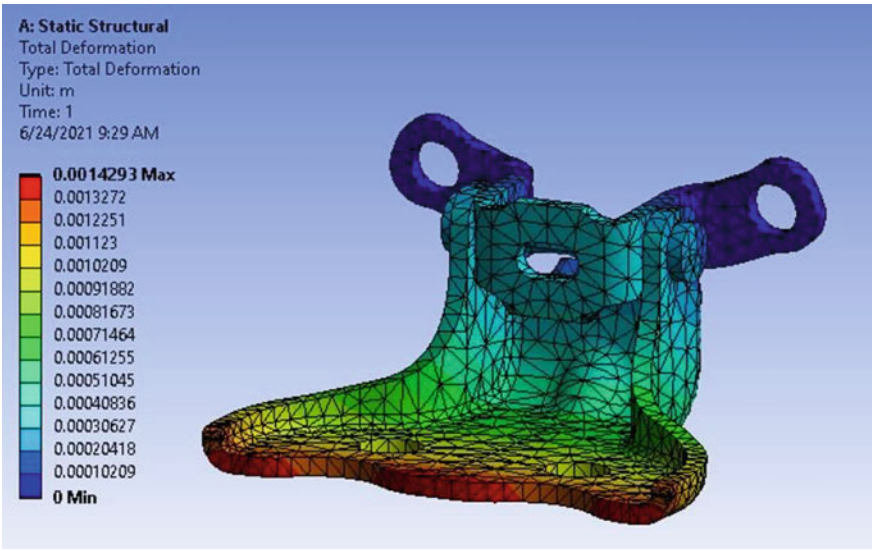

Fig. 6 Total deformation of car door hinge using cast iron material

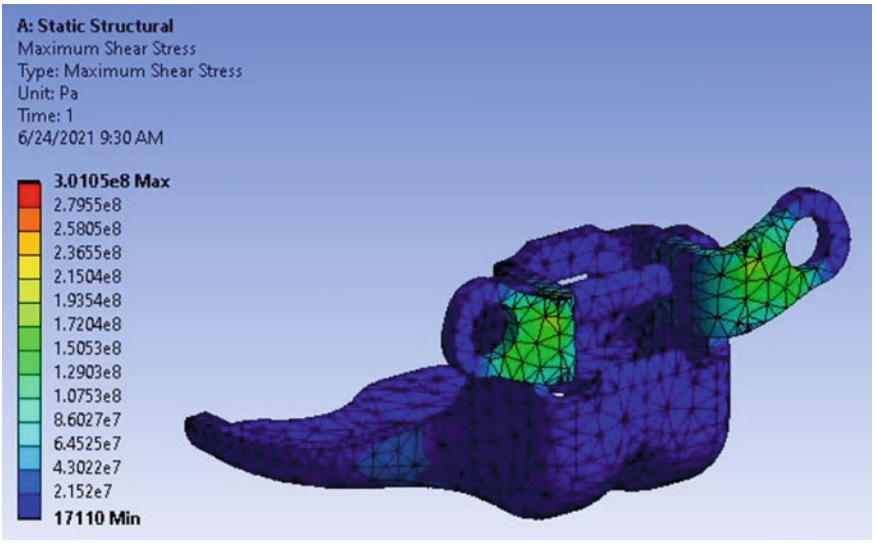

Fig. 7 Maximum elastic strain of car door hinge using aluminum material

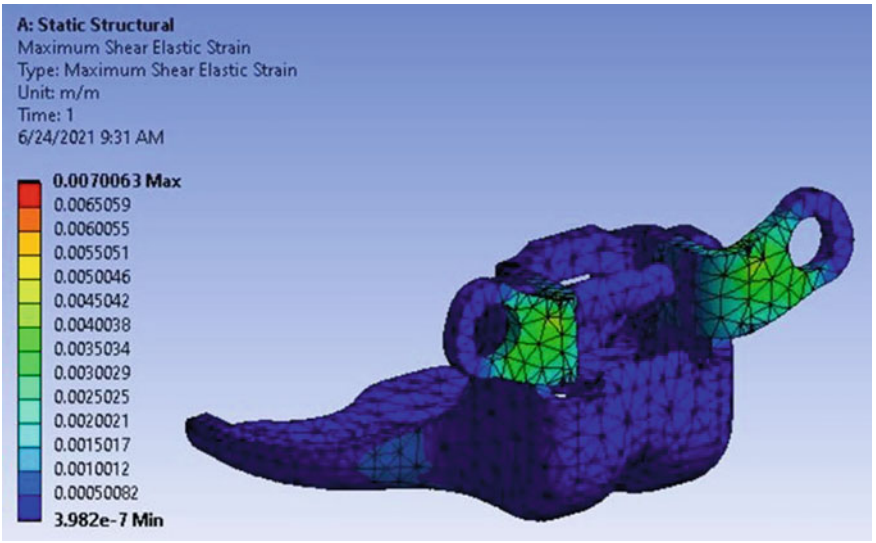

Fig. 8 Total deformation of car door hinge using cast iron material

Table 4 shows the comparison results between two materials. The maximum stress produced using aluminium alloy is exceeding the yield strength value. The yield strength for aluminium alloy is 2.8×10^8 Pa and the maximum stress produced is 2.9264×10^8 Pa. This indicates that the door hinge unable to withstand the maximum

Table 4 Comparison between aluminium and cast iron

Material	Aluminium	Cast Iron
Max. deformation	0.22402 mm	0.14293 mm
Max. stress produced	2.9264×10^8 Pa	3.0105×10^8 Pa

applied load of 400 N. For cast iron, it has zero yield strength in the same sense that there is no yield strength because it does not plastically deform. The maximum stress produced is compared with the ultimate strength of the material. The maximum stress produced for cast iron is not exceeding the ultimate strength. The ultimate strength for cast iron is 8.2×10^8 Pa and the maximum stress produced is 3.0105×10^8 Pa. This indicates that the door hinge could withstand the maximum applied load of 400 N.

Figure 9 shows the safety factor of the door hinge. The safety factor has a straightforward definition. It is defined as the ratio of the material's strength to the highest stress in the component. When the stress at a particular place exceeds the material's strength, the safety factor ratio falls below one, indicating that danger exists. It simply tells us that the stress in a certain location of the model is greater than the material's strength. When the stress in the model is significantly less than the material's strength, the safety factor is more than one, and the model is safe. From the results it shows that the minimum safety factor produced is very crucial since lowest value of safety factor is 0.1631.

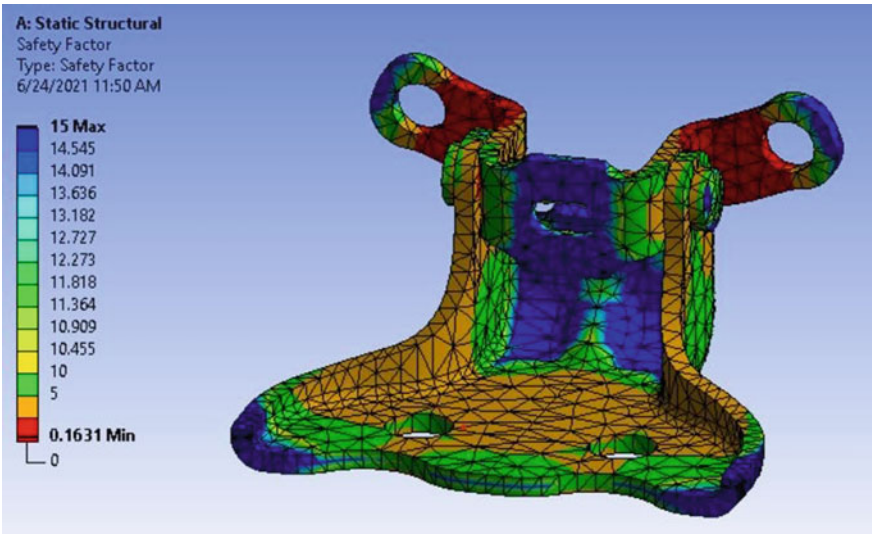

Fig. 9 Safety factor of car door hinge

4 Conclusion

The maximum stress and maximum displacement of the door hinge assembly were determined. The cast iron material shows the less deformation but higher stress compare with aluminium. Based on the yield strength and ultimate tensile strength of the both materials, door hinge made from cast iron is able to withstand the applied load. Thus, it can be concluded that cast iron material is preferable than aluminium.

Acknowledgements Authors would like to acknowledge the Ministry of Higher Education under Fundamental Research Grant Scheme FRGS/1/2019/TK03/UMP/02/21 (university reference RDU1901151) and Universiti Malaysia Pahang for financial supports.

References

1. Liu Z, Gao Y, Yang J (2021) Numerical and experimental-based framework for vibro-acoustic coupling investigation on a vehicle door in the slamming event. Mech Syst Sig Process 158:107759. https://doi.org/10.1016/j.ymssp.2021.107759
2. Liu Z, Gao Y, Yang J, Xu X, Fang J, Xu Y (2021) Effect of discretized transfer paths on abnormal vibration analysis and door structure improvement to reduce its vibration in the door slamming event. Appl Acoust 183:108306. https://doi.org/10.1016/j.apacoust.2021.108306
3. Oliver-Ortega H, Julian F, Espinach FX, Tarrés Q, Ardanuy M, Mutjé P (2019) Research on the use of lignocellulosic fibers reinforced bio-polyamide 11 with composites for automotive parts: car door handle case study. J Clean Prod 226:64–73. https://doi.org/10.1016/j.jclepro.2019.04.047
4. Liu Z et al (2021) Transfer path analysis and its application to diagnosis for low-frequency transient vibration in the automotive door slamming event. Measurement 183:109896. https://doi.org/10.1016/j.measurement.2021.109896
5. Cheon S, Jeong H, Hwang SY, Hong S, Domblesky J, Kim N (2015) Accelerated life testing to predict service life and reliability for an appliance door hinge. Procedia Manuf 1:169–180. https://doi.org/10.1016/j.promfg.2015.09.082
6. Soo VK, Compston P, Doolan M (2016) Is the Australian automotive recycling industry heading towards a global circular economy?—a case study on vehicle doors. Procedia CIRP 48:10–15. https://doi.org/10.1016/j.procir.2016.03.099

Graphene as an Alternative Additive in Automotive Cooling System

Ganesaan Kadirgama, Muhammad Izdihar Bin Razman, Devarajan Ramasamy, Kumaran Kadirgama, and Kaniz Farhana

Abstract The project represents graphene can be used as an alternative additive in the automotive cooling system. Thus, graphene nanofluids have been prepared at 0.1, 0.3 and 0.5% volume concentrations. Afterward, measurement of various thermophysical properties of nanofluid such as thermal conductivity, density, viscosity, and specific has been done. The obtaining data has been analyzed and compared with graphene oxide, titanium oxide, aluminium oxide, silicon carbide, and copper oxide nanofluid to figure out the best nanofluid that can absorb more heat to protect the car engine from overheating. In, summary, the overall best nanofluid among these six would be graphene oxide, with the best thermal conductivity, specific heat capacity, and one of the lowest viscosities. As for comparison among graphene all volume concentrations, the 0.1% graphene nanofluid demonstrated the best with high thermal conductivity and low viscosity.

Keywords Graphene · Nanofluid · Radiator · Automotive cooling system · Comparison

1 Introduction

The engine is the most critical component of the vehicle, and the control of the automobile and the drive of the car air conditioners are both powered by the engine, but the performance of the temperature engine that is too high will also reduce harm and the temperature of the engine that is too low can again increase the consumption

G. Kadirgama · M. I. Bin Razman · D. Ramasamy · K. Kadirgama
Faculty of Mechanical and Automotive Engineering Technology, Universiti Malaysia Pahang, 26600 Pekan, Pahang, Malaysia

K. Kadirgama
Center of Automotive Engineering, Universiti Malaysia Pahang, Pekan, Pahang, Malaysia

K. Farhana (✉)
Department of Apparel Engineering, Bangladesh University of Textiles, Dhaka 1208, Bangladesh
e-mail: kaniz.farhana@butex.edu.bd

M. Y. Ismail et al. (eds.), *Technological Advancement in Mechanical and Automotive Engineering*, Lecture Notes in Mechanical Engineering,
https://doi.org/10.1007/978-981-19-1457-7_2

of oil. Therefore, the successful guarantee of ensuring that the engine runs well below normal working temperatures is a cooling device [1].

In addition to the constant expansion of the business engine, the cooling fluid used to match it has also made considerable progress. On the market, current cooling fluid is all containing water coolant (substantially water, ethylene glycol), its boiling point is low, the freezing point is high, fast erosion of cavitation, weak heat conductivity, a significant volume of water vapor is not satisfied with the market requirement. For example, generating water coolant from the steam in the metallic surface of the cylinder periphery, causing timely engine work heating to take place in time, eventually overheating the engine interior and causing its deterioration, and permanent use of water coolant may also trigger corrosion to occur in the cooling system, incrustation scale, the series of problems such as boiling, causing the cooling system to foretell 2 years needs to change once [2, 3].

An atom-thick honeycomb layer of carbon atoms is known as graphene. Because a typical carbon atom has a width of about 0.33 nm, there are about 3 million layers of graphene in 1 mm of graphite, making it the building block for other graphitic materials. Nanographene is a type of graphene that is tailored to certain functions and so has a more complicated manufacturing process than regular graphene. Dehydrogenation is the process of selectively removing hydrogen atoms from organic carbon and hydrogen molecules to produce nanographene. Graphene is tougher than steel but lighter than aluminium, and it is harder than diamond but more elastic than rubber. Graphene is known as one of the strongest substances [4] has been extensively examined. Commercial use of materials and devices based on graphene. Various methods of preparing graphene have been developed to date, which can be divided into chemical vapor deposition of graphene layers, micromechanical exfoliation of graphite using the Scotch-tape peel-off method, epitaxial graphene foils, biomethane synthesis of organic molecular graphene, and GO sheets reduction or deoxygenisation [5]. In the case of using a CNC machine, lubricant mixed with water is used to cool and lubricate the tool and workpiece. It also transports the chip, contaminants, and debris away from the cutting area. Base grease is one of the materials used in lubricants. By adding graphene, it will enhance the tribological properties and thermal conductivity of base grease. In this study, the cooling performance of automotive has been investigated by using graphene nanofluids in various concentrations. Therefore, various thermophysical properties of graphene nanofluids such as thermal conductivity, density, viscosity, and specific heat have been studied comprehensively along with analogy of other's studies.

2 Literature Review

2.1 Graphene

In this research, graphene is the most important component as it acts as the additive in the cooling system. The best way to explain graphene is that it is the soft, flaky substance used in pencil lead, a thin and single layer of graphite. Graphite is the rhinestone of carbon element, which means it is constructed with the same atoms, but the crystal arrangement is different, providing different characteristics to the substance. Diamond and graphite, for example, are both sources of carbon, but they have wildly different natures. Although graphite is fragile, diamonds are extremely solid. The atoms of graphene are structured in a hexagonal structure. Interestingly, it takes on certain miraculous properties when graphene is removed from graphite. It is a simple one-atom-thick, the first-ever discovered 2D substance. Regardless of this, kits knew that graphene is also one of the strongest materials. With 130 GPa (gigapascals) of tensile strength, it is more than 100 times stronger than steel. Despite being so thin, graphene's incredible strength is already enough to make it impressive, but its special properties do not stop there. It is also pliable, translucent, superb conductive, and most fluids and gases are seemingly impermeable. It seems almost as if there is no region in which graphene does not excel [6–8].

2.1.1 Graphene Synthesis by Mechanical Exfoliation

The 2D research explosion as a catalyst has been separated from bulk graphite atomically into thin layer materials called graphene in 2004. Sir Konstantin Novoselov and Sir Andre Geim had won the 2010 Nobel Prize in the Physics area for their pioneering task on graphene in this seminal paper and subsequent research. As stated in Sir Andre Geim's Nobel speech, the research outcomes graphene attracted more attention due to its higher electronic efficiency, stability, and tunability at ambient temperatures that are vulnerable to the surroundings. Besides, unlike any other materials, the capability to achieve a broad mean free electron route at submicron distances without dispersion in before isolated graphene Hall bar mechanism that was attached to a microscopically harsh substance encircled by adsorbates and polymer residue was dissimilar with other substrates. Geim addresses surface science in the Nobel Lecture and how to study thin films involves a high vacuum, where properties usually decline as the thickness of material reduces; but this was not the case when Geim and his research group illustrated the effect of the electric field in FLG and began the boom of graphene and two-dimensional material [9, 10].

To describe the emerging optical properties comprehensively, the researchers researched the properties of bulk HOPG samples such as time-resolved reflectivity and time-resolved transmission across fragile samples. They measured the electronic carriers in solid graphite using a 50-fs pump and probe method over a broad range of optical agitation conditions but lower the threshold for the damage of optical

conditions. Significant scattering of light was found on the free-standing films while processing the samples, so the samples were taped to glass material, and the tape was then detached, minimizing the light scattering, leaving "mounted films" behind. The mechanical exfoliation strategy takes shape via Scotch tape, but it will not be until 14 years later that the strategy is utilized again to segregate, classify, and describe the effect of the single to FLG ambipolar electric field [9, 11].

The mechanical graphene exfoliation process known as the Scotch tape technique invented in 2004; is simply attaching tape to the surface of some form of bulk graphite, removing the tape away, and then adhering the tape and residues to a material, typically silicon oxide. The tape is pulled off until adhered to the substrate, and a final step of exfoliation leaves behind casually spaced flakes of different thicknesses, specifically monolayer graphene. But, in isolating FLG, the procedure conducted by Geim and Novoselov was quite interesting. To build mesas 5 μm in-depth in square form from 20 μm to 2 mm while the process begins by using an oxygen plasma etch of 1 mm thick HOPG platelets. The etched HOPG was then flipped and dipped on top of the glass into a wet photoresist of 1 μm thick. To solidify the photoresist and catch the mesas, the accumulation is then dried and cured. In phase 4, the dense layer of HOPG staying above the mesas is separated off, remaining the collection of mesas ingrained in the cured photoresist behind. It is in phase 5 where the renowned "Scotch tape process" is introduced. To deduct the number of HOPG layers connected by weak Van der Waals forces step by step, scotch tape is employed frequently to exfoliate mechanically the mesas fixed in the photoresist. The graphite mesas that are mechanically exfoliated are then put in an acetone dip, by dissolving the photoresist in acetone, releasing the flakes. In the water, the glass separates, remaining graphitic flakes in the acetone dip float. In step 7, along with the thin flakes of graphite, a silicon oxide layer material (n^+ doped) of 300 nm is immersed in the acetone dip. With water and propanol, the SiO_2 substrate is stripped and cleaned. Steps 7 and 8 are a single stage where the layer has been immersed, removed as shown in Fig. 1, and then washed with water and propanol in the solution. The water aids catch the narrow flakes on the material in this process. The material is put in a bath of ultrasound of propanol in the final stage, where added ultrasound cleaning eliminates bigger flakes and proceeds to narrow the graphite to possible FLG (~1–3 layers). Flakes below 10 nm thick were found to bind firmly to the SiO_2 surface by VDW and capillary forces, following the material. Lastly, from the ultrasound bath, the SiO_2/graphene composite is extracted, dried, and prepared for fabrication and characterization of the unit [9, 12].

The absorption of water between the occupied FLG graphene films and the SiO_2 substrate is referred to as a "dead sheet," presented in the recording of a standard 1 nm thickness greater than the original graphite interlayer spacing of 0.335 nm. It was successfully isolated and tested the electronic properties of graphene by Geim and his research group who used this mechanical exfoliation technique, even though many scientists who studied the material earlier had made substantial investigations with just a few layers of graphite [9, 13].

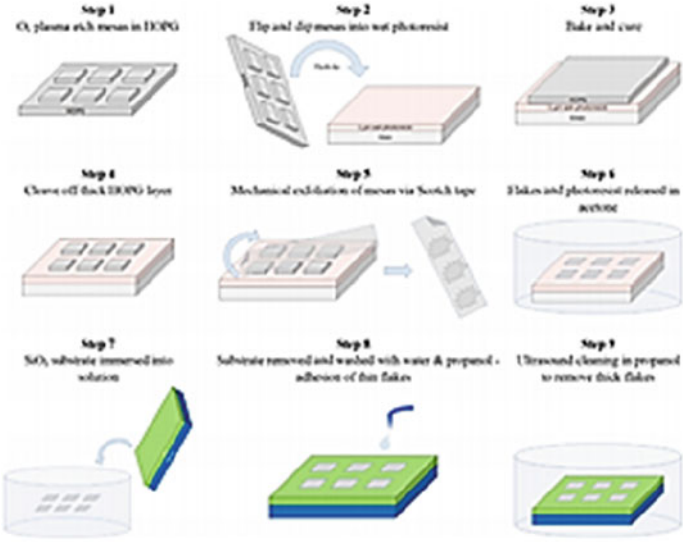

Fig. 1 Mechanical exfoliation of single to few-layer graphene for the measurements of the effect of the electric field in isolation ambipolar by using HOPG and associated microfabrication steps, determined in supporting substance of highly aligned pyrolytic graphite [9]

It was monumental to separate single to few-layer graphene. To determine the superb properties of this new substance at just a few atomic layers, however, electrical measurements were required. To describe the device structure, Hall bar devices with multiterminal were microfabricated using electron-beam lithography. Next, an O_2 plasma etch was used to remove undesirable substrate, connections were established using deposition and lithography of Au (100 nm) on Cr (5 nm) to clean the photoresist polymer using the final lift-off technique. This newly segregated FLG, with 10,000 cm^2/Vs mobilities, $n \approx 5 \times 10^{12}$ cm^{-2} charge density, and mean-free-path of electrons ~0.4 μm, all at room temperature, was involved in exposing the high electronic efficiency and tunability of multiterminal Hall bar devices. The characteristics were exceptional, especially regarding the existence of pollutants and the connected interface with the SiO_2 material. Enhancements in the transport of electrons were illustrated by encapsulated graphene in hexagonal boron nitride (HBN) on two sides, at low and room temperatures, with electrons ballistic transport (no scattering) [9, 14].

2.1.2 Graphene Synthesis by Chemical Vapor Deposition (CVD)

To synthesis graphene by the CVD method, the experimental setup was prepared by using a quartz tube housed within a furnace, precursor (argon and hydrogen), and nucleation (methane) gases, mass flow controllers, and a vacuum pump to control

low-pressure conditions. The graphene growth recipe is based on the material used and calibrated to the parameters of the experiment. To dissolve the hydrocarbon gas methane into its integral elements of carbon and hydrogen, high temperature is used, where the surface of the copper is covered with the interactions and depositions of carbon. The carbon atoms reorganize and crystallize during the cooling process to build hexagonal shapes derived from nuclear sites. The actual conditions for the recipe will spread grain fronts to laterally extend and consolidate to produce a continuous sheet (polycrystalline structure). Described by the Ruoff research community, the graphene growth method details the steps of growth of graphene domain on a copper foil. The pressure, time, temperature, and gas flow rates inside the growth tube or chamber mediate the graphene grains or domain size [9, 15, 16].

2.1.3 Thermal Conductivity of Graphene

Thanks to the remarkable properties of heat conductivity of graphene and its potentiality to apply in thermal control utilization, thermal transport in graphene is a flourishing area of study. At room temperature, the general thermal conductivity of graphene within a range of 3000–5000 Wm^{-1} K^{-1}, an outstanding rate compared with the thermal conductivity of pyrolytic graphite at room temperature of about 2000 Wm^{-1} K^{-1}. Other studies, however, state that this amount is extravagant and that graphene's thermal conductivity in-plane form for freely suspended samples at room temperature is around 2000–4000 Wm^{-1} K^{-1}. This figure is still among the largest of any substance known [17, 18].

Graphene is studied as an outstanding conductor of heat, and many investigations have revealed it to have limitless heat conduction capacity based on the sample size, contradicting the micrometer scale of Fourier's law. The researchers found, in both numerical simulations and experiments, that the bigger the graphene fragment could transfer more heat. Graphene could potentially consume an infinite quantity of heat. Logarithmically, increasing thermal conductivity happened due to the stable bonding pattern as like 2D material. Since graphene is substantially stronger than steel to tear and is also fragile and versatile, there may be some attractive real-world applications for its conductivity [17].

Electronics applications based on graphene-enabled thermal management could be vital beneficial from the ability of graphene to expend heat and maintain electronic operation. For smaller and more powerful devices, heat is also a specific factor in micro and nanoelectronics. Thus, for this form of application, graphene and alike materials with excellent thermal conductivity can hold immense promise. The heat conductivity of graphene can be used in various forms, including heat spreaders, thermal interface materials (TIM), thermal greases, nanocomposites based on graphene, and so on [19]. The physical properties of base fluids (EG and water/EG) are tabulated in Table 1 and the properties of nanoparticles are enlisted in Table 2.